

STUDY OF HYDRATION PRODUCTS IN THE MODEL SYSTEMS METAKAOLIN–LIME AND METAKAOLIN–LIME–GYPSUM

#MATÚŠ ŽEMLIČKA***, EVA KUZIELOVÁ**, MARTA KULIFFAYOVÁ**, JAKUB TKACZ***,
MARTIN T. PALOU**

*Faculty of Chemical and Food Technology, Slovak University of Technology,
Radlinského 9, SK-812 37 Bratislava, Slovak Republic

**Institute of Construction and Architecture, Slovak Academy of Sciences,
Dúbravská cesta 9, SK-845 03 Bratislava, Slovak Republic

***Materials Research Centre, Faculty of Chemistry, Brno University of Technology,
Purkyňova 118, CZ-612 00 Brno, Czech Republic

#E-mail: matus.zemlicka@stuba.sk

Submitted March 30, 2015; accepted October 19, 2015

Keywords: Blended cements, Metakaolin, Gypsum, Ettringite

Possible preferential formation of ettringite instead of required calcium silicate hydrate (CSH) and calcium aluminosilicate hydrate (CASH) phases when aluminosilicates were added to the blended cements was investigated on the model systems comprising of metakaolin, lime and gypsum. Compressive strength, microstructure and phase composition of the samples were evaluated after 7 days of curing at 50°C, using thermal analysis, X-ray diffraction techniques and scanning electronic microscopy. Samples prepared from equal amounts of metakaolin, lime and with more than 8 wt. % of gypsum, displayed the highest compressive strength values. Development of compressive strength was correlated with the formation of ettringite. Further rising of gypsum content resulted in the decrease of compressive strength, which is notable in the samples with a different metakaolin/lime ratio. Lower content of gypsum led to the preferential formation of portlandite, CSH and CASH. Calcite was detected in all the samples and its content declined with increasing amount of ettringite. In addition to calcite, carboaluminates were detected in complementary binary metakaolin - lime system. Tendency to carbonation declined with increasing content of metakaolin and eventuated in the highest compressive strength value for the samples with equal initial content of metakaolin and lime.

INTRODUCTION

The production of traditional cement is generally accompanied by high energy and limestone based material consumption. In the last decades, an enormous effort to reduce the carbon footprints together with a demand for improved materials has led to the development of so-called blended cements implying the use of alternative materials [1-3].

One of the most often applied supplementary cementitious materials in the recent years is metakaolin [4-9]. Metakaolin is usually added to blended cements in amount of 5 - 15 wt. %. It enhances long-term strength of concrete mixture, refines pore structure and thereby decreases permeability and improves resistance to soluble chemicals (sulfates, chlorides, acids) [4-8]. Pozzolanic activity of metakaolin and its effect on the properties of blended Portland cement has been subject of many reports [9-13]. Owing to its fineness and content of penta-coordinated aluminum ions that are formed during hydration process, metakaolin is very reactive and consumes portlandite ($\text{Ca}(\text{OH})_2$; which does not contribute to the strength and durability of concrete) by

formation of additional binding phases – calcium silicate hydrate (known as CSH), C_4AH_{13} ($2[\text{Ca}_2\text{Al}(\text{OH})_7 \cdot 3\text{H}_2\text{O}]$) [14], C_3AH_6 ($\text{Ca}_3[\text{Al}(\text{OH})_6]_2$) and C_2ASH_8 (stratlingite, $\text{Ca}_2\text{Al}_2\text{SiO}_7 \cdot 8\text{H}_2\text{O}$) [15, 16, 17]. The formation of crystalline products depends mainly on the AS_2/CH ($\text{Al}_2\text{Si}_2\text{O}_7/\text{Ca}(\text{OH})_2$) ratio and reaction temperature [18].

The reaction of Al_2O_3 from metakaolin (or other pozzolans) with sulfate bearing compounds in aqueous environment containing calcium ions can lead to the formation of ettringite ($\text{Ca}_3\text{Al}_2(\text{SO}_4)_3(\text{OH})_{12} \cdot 26\text{H}_2\text{O}$) [19]. Calcium sulfates (such as gypsum) are normally present in blended cement as inhibitors of setting. They regulate early hydration reactions to prevent fresh setting, improve strength development at earlier period and reduce drying shrinkage.

The primary source of ettringite formation in blended systems is reaction between the same calcium sulfate sources and clinker minerals like C_3A ($\text{Ca}_3\text{Al}_2\text{O}_6$) and C_4AF ($\text{Ca}_4\text{Al}_2\text{Fe}_2\text{O}_{10}$). Reaction takes place very fast after mixing with water. X-ray peaks of ettringite are detectable already within a few hours and increase in intensity to a maximum in approximately 1 day resulting in early strength of concrete [20].

Despite this, it was demonstrated that the formation rate of ettringite deriving from the reactive alumina in pozzolans is even higher than that from C₃A and much higher than from C₄AF [21]. According to the mentioned sources of formation, ettringites were termed as rapid (ett-rf), slow (ett-lf) and very slow formation (ett-vlf) [21-23]. Besides formation rate, ettringites originated from different sources differ in sizes, inter-relations and inter-connections occurred during hydration [23].

All of these parameters have technology impact and they should motivate the demand for investigation of ettringite development in these systems in more detail.

In the present study, the ternary model system containing metakaolin, lime and gypsum was selected and studied in order to elucidate the hydration reactions taking place in the considered types of blended metakaolin cements known as pozzalonic ones. Obtained results can help to select appropriate compositions of blended cements when CSH and CASH phases instead of ettringite are desired to be formed as dominant hydration products.

EXPERIMENTAL

Particular compositions of binary and ternary mixtures depicted in wt. % are shown in Table 1. Samples were prepared from limestone (quarry Konopiska, Rohožník, Slovakia, calcinated at 1100°C for 1 h), metakaolin L₀₅ (Mefisto, České lupkové závody, Czech Republic) and gypsum (Spišská Nová Ves, Slovakia) mixed together. Lime and gypsum were milled for 10 min in agate mill and sieved (mesh size 90 μm) before use.

All the 25 ternary samples were divided into five series (Table 1). In each series, the quantity of gypsum was gradually raised from 8.33 wt. % to 41.67 wt. % along with the unchanged ratio metakaolin/lime. In addition,

five binary samples consisting of metakaolin and lime were prepared for comparison. The amount of water was except two samples maintained constant (40 wt. %). In the samples 21 and 22, the water demand was increased to 49 % and 45 % respectively, owing to improvement of workability.

After adding of water, the mixtures were homogenized for 5 minutes. Homogenized samples were placed into the 2 cm cube moulds and cured above water for 7 days in the heating chamber. The temperature of 50°C was selected in order to accelerate hydration reactions. Subsequently after compressive strength measurements were performed, hydration of samples was stopped by immersing them in acetone. Residual acetone was removed by evaporating for 2 h at 50°C and samples were submitted to other analyses.

Compressive strength of hardened samples was estimated using WPM WEB Thuringer Industriewerk Raustein 11/2612 (up to 25 000N). Each displayed data represents arithmetic mean of 6 experimental measurements. The presence of crystalline phases in the samples was evaluated by XRD analysis (STOE theta/theta diffractometer, Siemens Germany; CoK α radiation, $\lambda = 0.179$ nm, operating at 40 kV and 30 mA). Microstructure of samples was analyzed by SEM (JEOL JSM-7600F, max. resolution of 0.8 nm). Crystal morphology of individual phases was determined by microanalysis. Electron Probe Micro Analyzer JEOL JXA-840A (EDS parameters – 15 KV, Takeoff Angle 40.0°) was used. All the samples selected for microanalysis were carbon coated. In order to determine the phase changes, thermal analysis was used (TGA/DSC – 1, STARe software 9.30, Mettler Toledo). The 50.00 (± 0.03) mg of powdered samples was heated in the open platinum crucibles up to 1000°C at the heating rate of 10°C·min⁻¹ in the atmosphere of synthetic air (purity 5.0).

Table 1. Labelling of samples prepared from ternary and binary compositions.

Series	I.					II.					III.				
	5					2					1				
Metakaolin/Lime ratio															
Sample	1	2	3	4	5	6	7	8	9	10	11	12	13	14	15
Gypsum (wt. %)	8.33	16.67	25.00	33.33	41.67	8.33	16.67	25.00	33.33	41.67	8.33	16.67	25.00	33.33	41.67
Metakaolin (wt. %)	76.33	69.50	62.50	55.50	48.67	61.17	55.50	50.50	44.50	38.83	45.83	41.67	37.50	33.33	29.17
Lime (wt. %)	15.33	13.83	12.50	11.17	9.67	30.50	27.83	25.00	22.17	19.50	45.83	41.67	37.50	33.33	29.17

Series	IV.					V.					B.				
	0.5					0.2					5	2	1	0.5	0.2
Metakaolin/Lime ratio															
Sample	16	17	18	19	20	21	22	23	24	25	B _I	B _{II}	B _{III}	B _{IV}	B _V
Gypsum (wt. %)	8.33	16.67	25.00	33.33	41.67	8.33	16.67	25.00	33.33	41.67	0.00	0.00	0.00	0.00	0.00
Metakaolin (wt. %)	30.50	27.83	25.00	22.17	19.50	15.33	13.83	12.50	11.17	9.67	83.33	66.67	50.00	33.33	16.67
Lime (wt. %)	61.17	55.50	50.00	44.50	38.83	76.33	69.50	62.50	55.50	48.67	16.67	33.33	50.00	66.67	83.33

RESULTS AND DISCUSSION

Binary samples

XRD analyses

In general, two kinds of competitive reactions can occur in binary metakaolin – lime systems. The first one is reaction of metakaolin with calcium hydroxide leading to CSH gel, several calcium aluminosilicate hydrates (such as C_2ASH_8) and calcium aluminate hydrate (C_4AH_{13} , etc.). The second type is carbonation. According to Massazza [24] and Vénuat *et al.* [25] the reaction rates of both pozzolanic and carbonation reactions depend on temperature and relative humidity during curing. Whereas high temperatures and saturated relative humidity favor the pozzolanic reaction, relative humidity values of around 60 % favor carbonation.

Curing of binary samples at 50°C and 95 % of relative humidity were led to the significant carbonation. In addition to calcite ($CaCO_3$), also monocarboaluminate ($C_4\bar{A}CH_{11}$, $Ca_4Al_2CO_9 \cdot 11H_2O$) was detected on particular XRD patterns (Figure 1). Monocarboaluminate arose from reaction of amorphous CASH, CSH gels and $Ca(OH)_2$ with atmospheric carbon dioxide. Unreacted portlandite was revealed only in the sample prepared from the highest content of lime. In samples with a high relative preliminary amount of metakaolin the presence of crystalline C_4AH_{13} along with monocarboaluminate were detected. Hydration of samples B_{III} and B_{IV} led also to the crystallization of hydrogarnet (C_3ASH_6). Whereas Silva *et al.* [26] attributed the formation of hydrogarnet to the transformation of metastable C_2ASH_8 and C_4AH_{13} under long curing, other authors [27] proved that hydrogarnet originates directly from the initial compounds. XRD analysis of samples B_I and B_{II} revealed besides carbonation products also stratlingite. Unreacted metakaolin was detected in these systems with higher metakaolin/lime ratio.

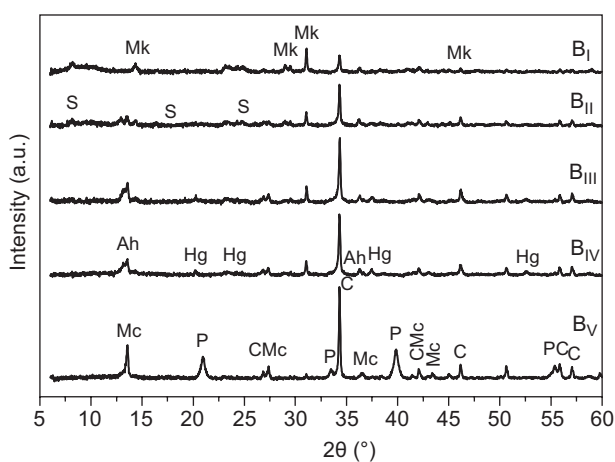


Figure 1. XRD patterns of samples from binary metakaolin–lime system (abbreviations: Mc – monocarboaluminate, Ah – C_4AH_{13} , Hg – hydrogarnet, P – portlandite, C – calcite, S – stratlingite, Mk – metakaolin).

Results of thermal analysis

Results of thermal analysis (Figure 2) correspond well with those of XRD patterns. Following the release of physically bonded water, the first significant endothermic peak appears between 140 - 200°C. It can be attributed to the decomposition of carboaluminates (according to XRD detected monocarboaluminate) [28]. Increasing preliminary amount of metakaolin in samples resulted in the disappearance of crystalline carboaluminates and their substitution by crystalline C_4AH_{13} and hydrogarnet on particular XRD patterns (Figure 1). Further rise of metakaolin content eventuated in the crystallization of stratlingite. Accordingly, intensity and range of the peak belonging to the carboaluminates decomposition decrease whereas peaks assigned to the decomposition of C_4AH_{13} (between 220 - 280°C [29]) and hydrogarnet series (280 and 360°C [30]) become more distinguished. Decomposition of stratlingite is evident from the presence of peak located between approximately 190 - 200°C [31, 32]. Strong peak assigned to the decomposition of portlandite (400 - 500°C) was detected only on the curve of sample with the lowest initial content of metakaolin (B_V) [33, 34]. Slight endothermic maximum of portlandite decomposition can be observed also in the case of sample B_{IV}. The thermal decomposition of calcite between 630 - 780°C presented the strongest endothermic maximum except samples B_{II} and B_{III} (with lower intensities in comparison with that of carboaluminates) [35]. All of above mentioned clearly demonstrates that carbonation is univocally preferred over the hydration reactions in the studied binary systems. The last S-shaped endothermic/exothermic effect at about 935°C can be attributed to the decomposition of calcite and the formation of mullite ($Al_6Si_2O_{13}$) [36].

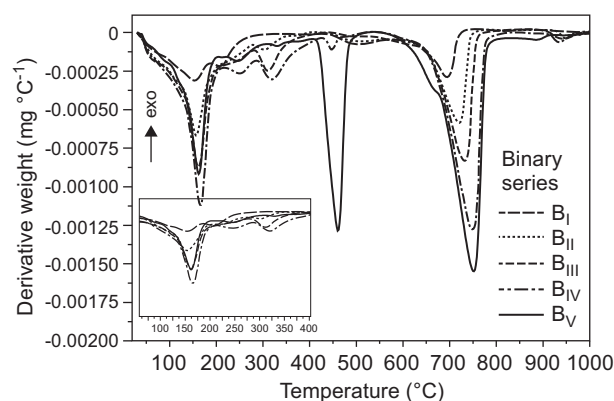


Figure 2. DTG curves of binary samples after 7 days curing at 50°C.

Compressive strength

Results of compressive strength are shown in Figure 3. The highest value of compressive strength was found for the sample prepared from the equal amounts of

metakaolin and lime. Increasing or decreasing quantity of metakaolin with regard to the lime content led to the gradual decrease of compressive strength.

Considering blended cements, there are three elementary factors influencing the contribution of metakaolin to the strength of final concrete: the filler effect, the acceleration of OPC hydration and the pozzolanic reaction of metakaolin with calcium hydroxide [37]. The filler effect of metakaolin which results in more efficient paste packing is according to Wild *et al.* [38] immediate and the acceleration of hydration was proved to have maximum impact within the first 24 h. The main factors influencing strength development in the binary systems are pozzolanic reaction, carbonation and their impact on the phase composition, microstructure and pore characteristics of final material. Higher compressive strength of sample B_{III} when compared to the samples B_{IV} and B_V is caused by its improved resistance to carbonation. This is confirmed by lower intensities of peaks belonging to calcite and carboaluminate on XRD as well as on DTA curves. As mentioned above, higher amounts of metakaolin in B_I and B_{II} led to the formation of stratlingite and further depletion of carbonation. Whereas stratlingite belongs to the strength bearing phases, lower compressive strengths of these samples can be attributed to the presence of unreacted metakaolin.

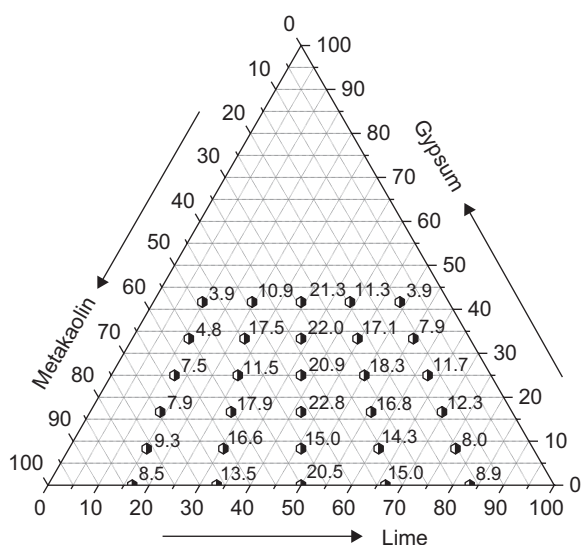


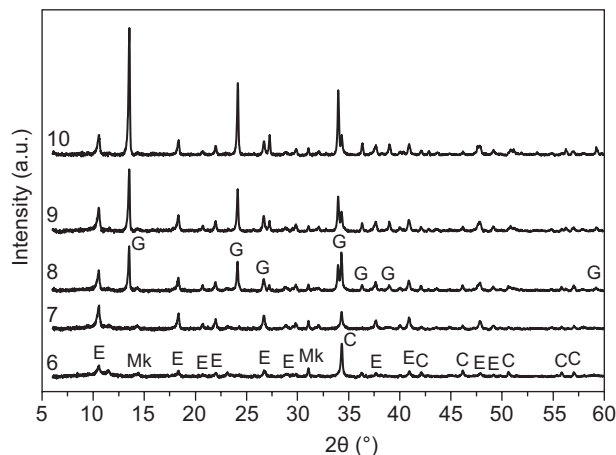
Figure 3. Results of compressive strength (MPa).

Ternary samples

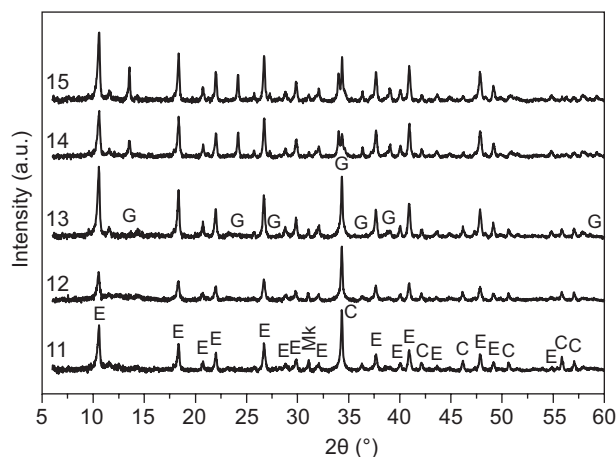
XRD analyses

XRD patterns of ternary samples from Series II., III. and IV. are shown in Figure 4. Ettringite and calcite were detected in all the samples composed preliminary of lime, metakaolin and gypsum. Quantity of hydration products depend on the relative proportions of input materials.

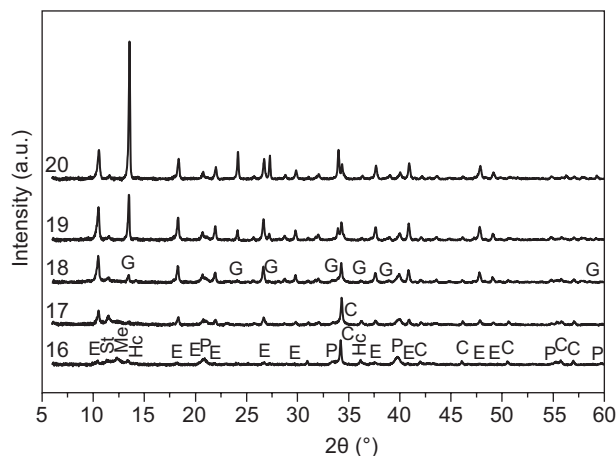
The content of ettringite corresponds well with the estimated values of compressive strength. As expected, compressive strength increased with increasing intensity of XRD peaks belonging to ettringite. Dermatas and Meng [39] have attributed significant strength gain of samples



a) Series II.



b) Series III.



c) Series IV.

Figure 4. XRD patterns of samples from Series II., III. and IV (abbreviations: E – ettringite, Hc – hemicarboaluminate, St – stellerite, Me – metaheulandite, Mk – metakaolin, P – portlandite, C – calcite, G – gypsum).

containing more ettringite to the crystal interlocking provided by its needle-like structure. When gypsum remained in the system partially unreacted due to its high initial quantity, values of 7 days compressive strength decreased. Lower contents of gypsum resulted in the preferential formation of CSH and CASH gels (in the case of Series IV. also portlandite), that due to their instability under the influence of carbon dioxide from the air underwent carbonation. Appropriately, intensity of peaks pertaining to calcite decreased with increasing ettringite, which was formed as more stable phase. Although the initial carbonation of portlandite is usually faster than that of CSH and CASH [40] its presence is unlike two later mentioned visible on all XRD patterns. This is caused by low crystallinity of particular phases. In addition, after some time the microcrystal layers of CaCO_3 form on the surface of $\text{Ca}(\text{OH})_2$ and carbonation of portlandite slows down [40]. Among many possible CSH and CASH phases that could accrue in the present systems, only crystalline stellerite ($\text{Ca}_2\text{Al}_4\text{Si}_{14}\text{O}_{36}\cdot 14\text{H}_2\text{O}$) and metaheulandite ($\text{Ca}(\text{Al}_2\text{Si}_7\text{O}_{18})\cdot 7\text{H}_2\text{O}$) were detected by XRD in the case of sample 16. Higher instability of emergent phases against carbonation led to the formation of hemicarboaluminate ($[\text{C}_4\text{Al}_2(\text{OH})_{12}][\text{OH}(\text{CO}_3)_{0.5}\cdot 4\text{H}_2\text{O}]$) in this sample.

Results of thermal analysis

DTG curves of the samples from Series II., III. and IV. are shown in Figure 5.

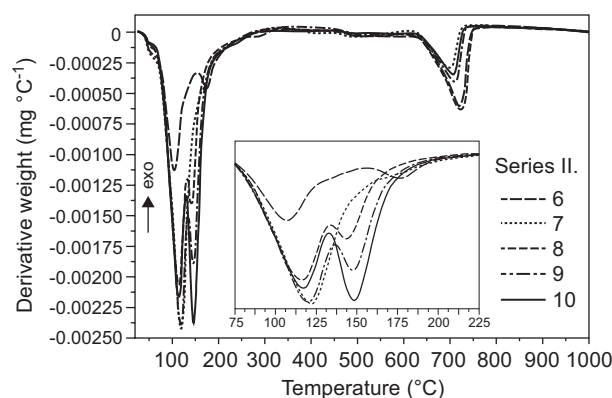
The first endothermic peak appearing, in the case of samples prepared with the lowest content of gypsum (8.33 wt. %), between 70°C and 135°C corresponds with the release of water due to decomposition of the nearly amorphous hydrates (mainly CSH) [33, 41]. The position of the first endothermic peak on the DTA curves of other samples (initially containing 16.67 wt. % and more gypsum) is moved to higher temperatures. The presence of this peak can be attributed to the combined effect of CSH and ettringite decomposition or merely to the ettringite [42]. Higher content of ettringite induces the shift of particular maximums to higher temperatures and increase of peak intensities which corresponds well with recorded XRD patterns (Figure 4).

The presence of unreacted gypsum in the samples prepared with 25.00 wt. % and more gypsum is evidenced using DTA technique by its decomposition that occurs in two steps (decomposition of dihydrate to hemihydrate between 135 - 180°C is followed by decomposition of hemihydrate to anhydrite between 180 - 215°C) [43]. Two mentioned endothermic peaks are on the presented DTA curves gathered together and extended approximately between 130°C and 180°C (with maximum at about 150°C).

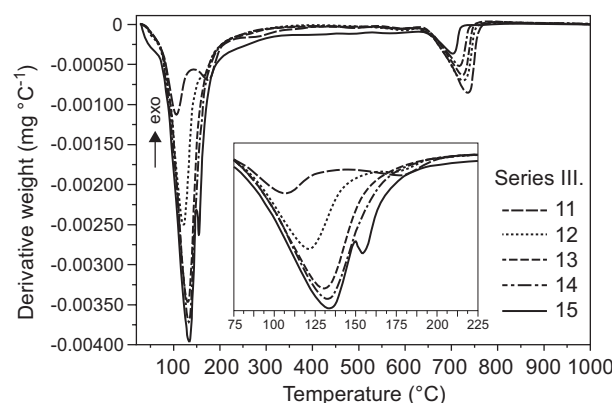
Following endothermic peak occurs between approximately 140 - 200°C and was detected only on DTA curves of samples containing initially higher amounts

of lime and lower amounts of gypsum. According to the results of binary systems analyses it can be attributed to the decomposition of carboaluminates.

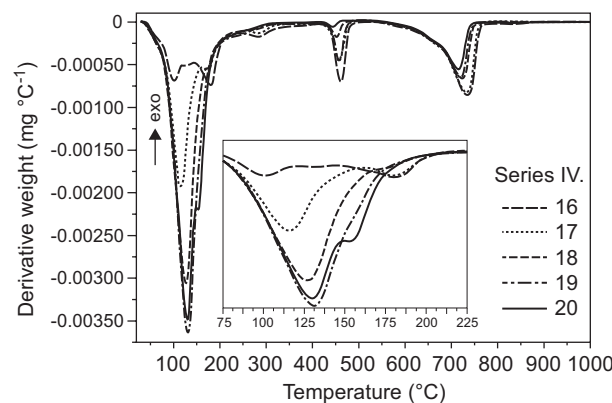
The decomposition of CASH phases is visible by small peaks between 250°C and 320°C on DTA curves [44, 45]. Among samples from Series II. and III. is this peak detected only on DTA curves of samples prepared with the lowest content of gypsum (8.33 wt. %). When more lime was used in preparation, the decomposition of CASH can be visible also on DTA curves of samples initially containing more gypsum.



a) Series II.



b) Series III.



c) Series IV.

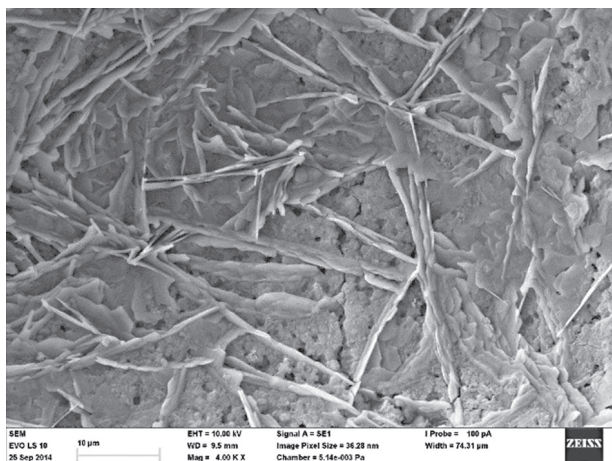
Figure 5. DTG curves of samples from Series II., III. and IV.

A sharp endothermic peak between 400°C and 500°C corresponding to the decomposition of portlandite into free lime [33, 34] was observed only on DTA curves of samples from Series IV. Decarbonation as a result of calcium carbonate decomposition is observed between 670°C and 750°C [35]. Except the

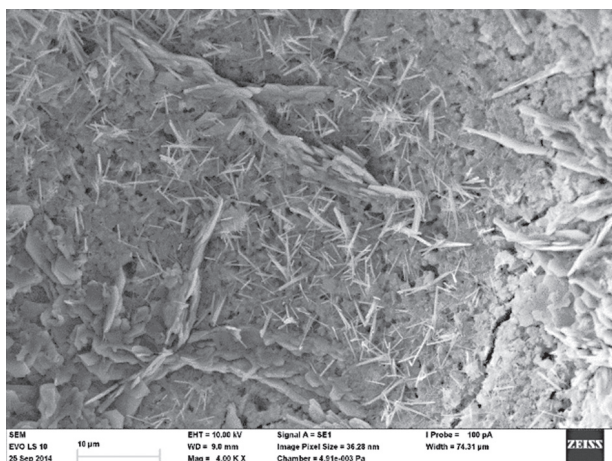
case when 25.00 wt. % of gypsum was used for preparation, maximum of particular peak moved to higher temperatures and high of peak increased with increasing content of lime. Maximum peak temperature and its intensity were not affected by initial metakaolin/lime ratio in the previously mentioned samples. The only exothermic peak occurring at approximately 980°C can be assigned to the mullite formation [46]. Its intensity is higher in the case of samples from Series II. (greater initial content of metakaolin) and did not appear on DTA curves of samples from Series IV. Accordingly, higher amount of lime in the samples from Series IV. are not beneficial for mullite formation.

Compressive strength

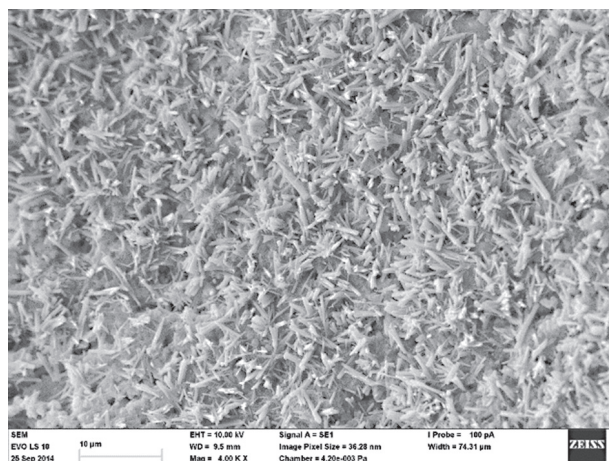
The highest values of compressive strength (above 20 MPa) displayed samples prepared with equal content of metakaolin and lime with gypsum content higher than 8.33 wt. % (Figure 3). As the metakaolin/lime ratio increased (Series I. and II.) or decreased (Series IV. and V.) towards the compositions of binary mixtures,



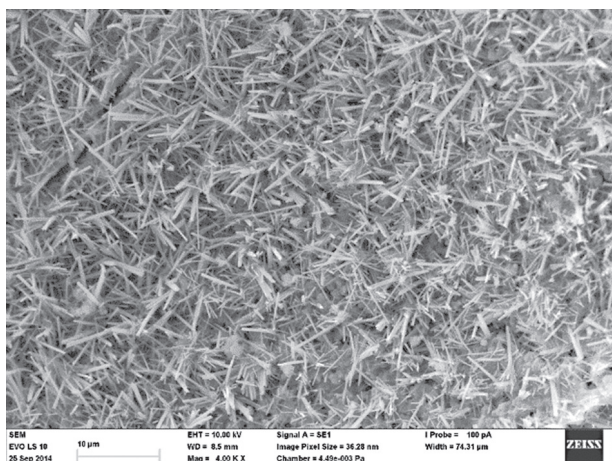
a) Sample 11



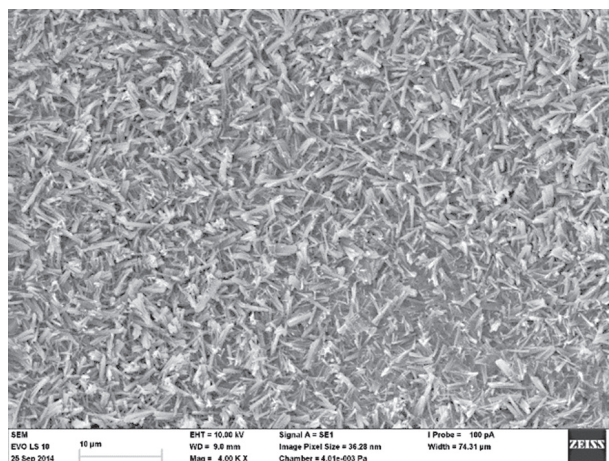
b) Sample 12



d) Sample 14



c) Sample 13



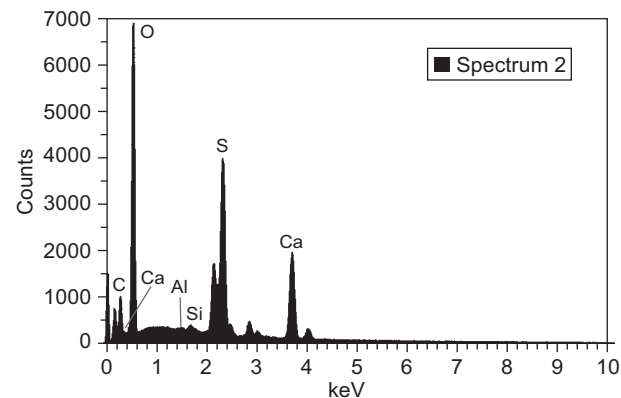
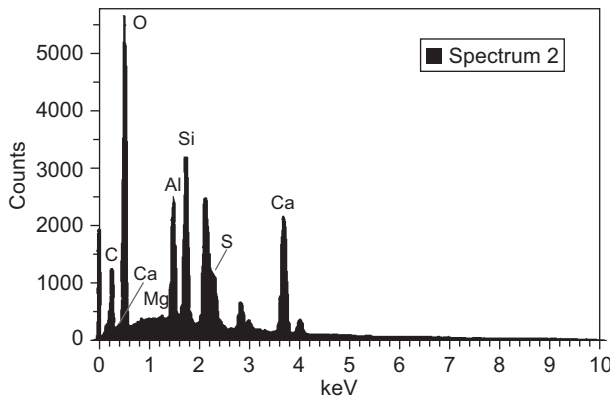
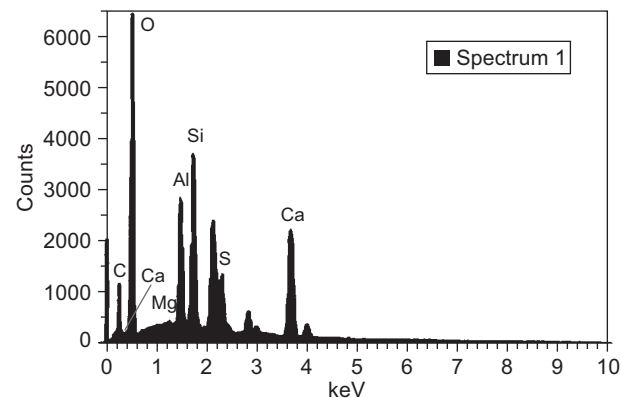
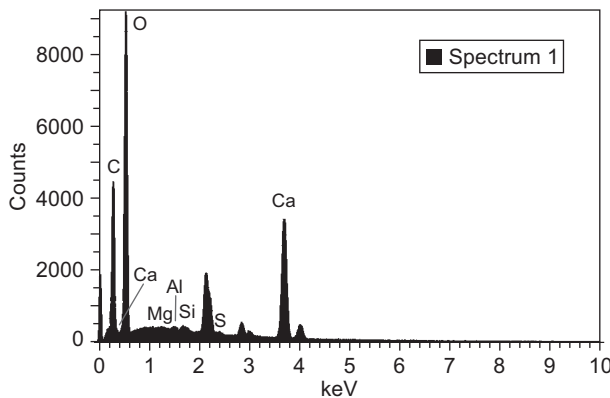
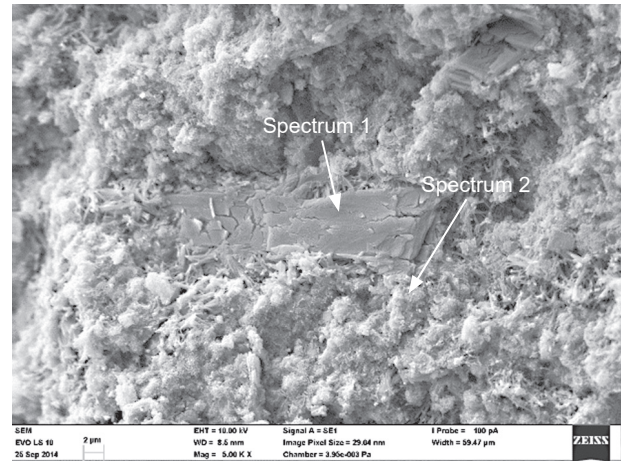
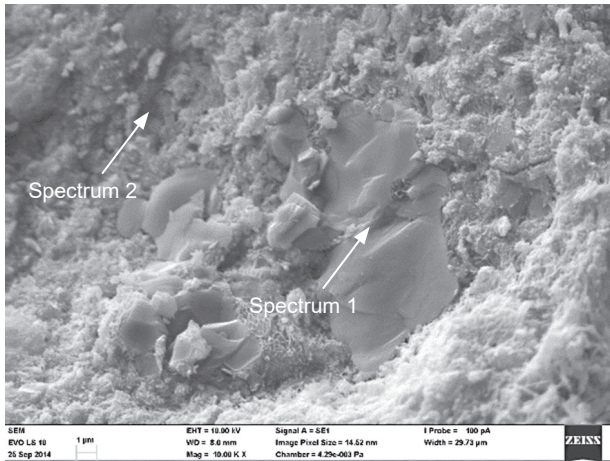
e) Sample 15

Figure 6. Needles of ettringite crystallized in the samples from Series III. (the scale bars represent 10 µm).

compressive strengths depleted. Higher gypsum quantity led to the decrease of compressive strength values, especially in the samples with bigger difference between metakaolin and lime quantity. Accordingly, the lowest values of compressive strength (3.9 MPa) were determined in the case of samples belonging to Series I. and II. and containing 41.67 wt. % of gypsum. The influence of gypsum on the compressive strength of all other Series is not so unequivocal.

SEM and EPMA analysis

The effect of higher gypsum content on the development of crystalline phases in Series III. is evident also from SEM micrographs (Figure 6) supported by electron probe microanalysis (Figure 7). The presence of ettringite is more obvious and its needle-like crystals become better developed as higher amount of gypsum was used to prepare particular samples. Besides ettrin-



a) Series III.; Sample 13

b) Series III.; Sample 15

Figure 7. Microstructure and relevant EDS spectra of samples belonging to Series III. and prepared with 25.00 wt. % (Sample 13; the scale bar represents 1 μm) and 41.67 wt. % of gypsum (Sample 15; the scale bar represents 2 μm).

gite, larger platelet crystal phases and column aggregates interspersed between finer phases appeared in all observed samples. According to the literature, hexagonal plate crystals that aggregate taking the form of column can be assigned to calcite [47]. This is supported also by EPMA microanalysis that assessed lower contents of Si, Al and S in such shaped crystals. In general, calcite can show variety of crystal habits (rhombohedra, tabular forms, prisms, scalenohedra) and its morphology and crystal size differ along the sample thickness [48]. In accordance with XRD analysis, prismatic crystals of unreacted gypsum were observed only on the SEM micrographs of the sample containing its highest initial amount (41.67 wt. %). Lower contents of Si, C and Al together with higher content of S and Ca/S ratio of 1.2 (close to 1.25 in pure gypsum) determined by EPMA microanalysis in particular places confirmed this statement.

Finer phases presented in all observed samples are composed of mixture of all mentioned elements in various ratios. Due to their low crystallinity they can be attributed mainly to CSH and CASH gels.

CONCLUSION

The presented study dealt with the possible preferential formation of ettringite in the cases that aluminosilicates are added to the blended cements. For this purpose, a model system comprising of metakaolin, lime and gypsum was selected and studied. When the equal amounts of metakaolin and lime were used to prepare samples, 8.33 wt. % of gypsum was sufficient to initiate ettringite formation prior to other hydration products. Precipitated crystals of ettringite possessed a needle-like shape as was documented by SEM analyses. Preferential formation of CSH and CASH phases in the systems with a higher or lower metakaolin/lime ratio was accompanied with substantial carbonation and lower compressive strengths. XRD supported by thermal analyses revealed that also unreacted gypsum was detected at its lower initial amounts when compared to the samples prepared with metakaolin/lime ratio equal to 1.

Samples belonging to the binary system displayed a significant carbonation. In addition to calcite, the presence of monocarboaluminate was demonstrated. Higher initial amounts of metakaolin reduced carbonation and resulted in higher compressive strength values. Maximum compressive strength was achieved for the sample with equal metakaolin/lime ratio. Further increase of the metakaolin content was demonstrated by the formation of stratlingite. The descent of compressive strength was probably caused by the presence of unreacted metakaolin that was detected in some particular samples.

According to the presented results, it can be deduced that the presence of aluminosilicates (such as metakaolin) and calcium sulfates in blended cements can

eventuate in the preferential formation of ettringite. The formation of required CSH and CASH binding phases can be attained by the appropriate adjustment of initial compounds amounts.

Acknowledgement

This work was supported by courtesy of the Slovak Grant Agency VEGA No. 2/0082/14 and by Project Sustainability and Development REG LO1211 addressed to the Materials Research Centre at FCH VUT.

REFERENCES

1. Snellings R., Mertens G., Cizer Ö., Elsen J.: *Cement Concrete Res.* 40, 1704 (2010).
2. Uzal B., Turanlı L.: *Cement and Concrete Composites* 34, 101 (2012).
3. Saca N., Georgescu M.: *Constr. Build. Mater.* 71, 246 (2014).
4. Roy D.M., Arjunan P., Silsbe M.R.: *Cement Concrete Res.* 31, 1809 (2001).
5. Hewayde E., Nehdi M. L., Allouche E., Nakhla G.: *Constr. Mater.* 160, 25 (2007).
6. Al-Akhras N.M.: *Cement Concrete Res.* 36, 1727 (2006).
7. Courard L., Darimont A., Schouterden M., Ferauche F., Willem X., Degeimbre R.: *Cement Concrete Res.* 33, 1473 (2003).
8. Khater H.M.: *Ceram-Silikaty* 54, 325 (2010).
9. Poon C.S., Kou S.C., Lam L.: *Constr. Build. Mater.* 20, 858 (2006).
10. Vejmelková E., Pavlíková M., Keppert M., Keršner Z., Rovnaníková P., Ondráček M., Sedlmajer M., Černý R.: *Constr. Build. Mater.* 24, 1404 (2010).
11. Wild S., Khatib J.M., Jones A.: *Cement Concrete Res.* 26, 1537 (1996).
12. Konan K.L., Peyratout C., Smith A., Bonnet J.P., Rossignol S., Oyetola S.: *J. Colloid Interf. Sci.* 339, 103 (2009).
13. Bich Ch., Ambroise J., Péra J.: *Appl. Clay Sci.* 44, 194 (2009).
14. Janotka I.: *Ceram-Silikaty* 45, 16 (2001).
15. Krajčí E., Janotka I., Puertas F., Palacios M., Kuliffayová M.: *Ceram-Silikaty* 57, 74 (2013).
16. Coleman N.J., McWhinnie W.R.: *J. Mater. Sci.* 35, 2701 (2000).
17. Changling H., Osbaeck B., Makovicky E.: *Cement Concrete Res.* 25, 1691 (1995).
18. Antoni M., Rossen J., Martirena F., Scrivener K.: *Cement Concrete Res.* 42, 1579 (2012).
19. Rahhal V., Talero R.: *Constr. Build. Mater.* 53, 674 (2014).
20. Evju C., Hansen S.: *Cement Concrete Res.* 35, 2310 (2005).
21. Talero R.: *Cement Concrete Res.* 26, 1277 (1996).
22. Talero R.: *Cement Concrete Res.* 33, 707 (2002).
23. Talero R.: *Cement Concrete Res.* 35, 1269 (2005).
24. Massazza F.: *Pozzolana and pozzolanic cements Lea's "chemistry of cement and concrete"*, p. 471-631, Ed. Hewlett Peter C., UK: Arnold 1999.
25. Vénuat M., Alexandre J.: CERILH no. 195, 1977.
26. Silva P.S., Glasser F.P.: *Cement Concrete Res.* 23, 627 (1993).

27. Rojas M.F.: *Cement Concrete Res.* 36, 827 (2006).
 28. Antoni M., Rossen J., Martirena F., Scrivener K.: *Cement Concrete Res.* 42, 1579 (2012).
 29. Saikia N., Kato S., Kojima T.: *Thermochim. Acta* 444, 16 (2006).
 30. Sepulcre-Aguilar A., Hernández-Olivares F.: *Cement Concrete Res.* 40, 66 (2010).
 31. Moropoulou A., Bakolas A., Aggelakopoulou E.: *Thermochim. Acta* 420, 135 (2004).
 32. Cabrera J., Rojas M.F.: *Cement Concrete Res.* 31, 177 (2001).
 33. Fares H., Remond S., Noumowe A., Cousture A.: *Cement Concrete Res.* 40, 488 (2010).
 34. Bažant Z.P., Kaplan M.F.: *Concrete at high temperatures*, Longman Addison-Wesley, London 1996.
 35. Matsushita F., Aono Y., Shibata S.: *Cement Concrete Res.* 30, 1741 (2000).
 36. Habert G., Choupy N., Montel J.M., Guillaume D., Escadeillas G.: *Cement Concrete Res.* 7, 963 (2008).
 37. Kadri E., Kenai S., Ezziane K., Siddique R., De Schutter G.: *Appl. Clay Sci.* 53, 704 (2011).
 38. Wild, S., Khatib, J.M., Jones, A.: *Cement Concrete Res.* 26, 1537 (1996).
 39. Dermatas D., Meng X.: *Eng. Geol.* 7, 377 (2003).
 40. Thiery M., Villain G., Dangla P., Platret G.: *Cement Concrete Res.* 37, 1047 (2007).
 41. Ibrahim I.A., ElSersy H.H., Abadir M.F.: *J. Therm. Anal. Calorim.* 76, 713 (2004).
 42. Portilla M.: *Cement Concrete Res.* 19, 319 (1989).
 43. Paulik F., Paulik J., Arnold M.: *Thermochim. Acta* 200, 195 (1992).
 44. Amin M.S., Abo-El-Enain S.A., Rahman A.A., Alfalous K.A.: *J. Therm. Anal. Calorim* 107, 1105 (2012).
 45. Amer A.A.: *J. Therm. Anal. Calorim.* 54, 837 (1998).
 46. Chakravorty A.K., Ghosh D.K.: *J. Am. Ceram. Soc.* 71, 978 (1988).
 47. Cultrone G., Sebastián E., Ortega Huertas M.: *Cement Concrete Res.* 35, 2278 (2005).
 48. Cizer Ö., Rodríguez-Navarro C., Ruiz-Agudo E., Elsen J., Van Gemert D., Van Balen K.: *J. Mater. Sci.* 47, 6151 (2012).
-